



PERGAMON

Available online at [www.sciencedirect.com](http://www.sciencedirect.com)

SCIENCE @ DIRECT®

Vacuum 71 (2003) 481–486

VACUUM  
SURFACE ENGINEERING, SURFACE INSTRUMENTATION  
& VACUUM TECHNOLOGY

[www.elsevier.com/locate/vacuum](http://www.elsevier.com/locate/vacuum)

# Patterning of Ru electrode in O<sub>2</sub>/Cl<sub>2</sub> gas using reactive ion etcher

Hyoun Woo Kim<sup>a,\*</sup>, Byong-Sun Ju<sup>b</sup>, Chang-Jin Kang<sup>b</sup>

<sup>a</sup> School of Materials Science and Engineering, Inha University, 253 Yong-Hyun-Dong, Nam-Ku, Incheon 402-751, South Korea

<sup>b</sup> Semiconductor R&D Center, Samsung Electronics, San 24 Nongseo-Ri, Kiheung-Eup Yongin-City, Kyungki-Do 449-711, South Korea

Received 27 November 2002; received in revised form 6 January 2003; accepted 20 February 2003

## Abstract

We have studied the reactive ion etching of Ru electrode using O<sub>2</sub>/Cl<sub>2</sub> plasma. We have revealed that the Ru etch rate and thus the Ru to SiO<sub>2</sub> etch selectivity increase by increasing pressure, total gas flow rate, temperature and decreasing the HRF power and LRF power. The vertical Ru etching profile is attained.

© 2003 Elsevier Science Ltd. All rights reserved.

*Keywords:* Ru; Etching; RIE; Etching profile

## 1. Introduction

As the dimension of devices decreases in size, high dielectric materials, such as barium strontium titanate (BST), tantalum pentoxide (Ta<sub>2</sub>O<sub>5</sub>), need to be used for the fabrication of dynamic random access memory (DRAM) capacitors [1–4].

Although platinum (Pt) has been usually investigated as an electrode material, Pt had an etching problem. Several research groups have reported that obtaining the sufficient etching selectivity of Pt to the mask material is very difficult [5–7]. On the other hand, ruthenium (Ru) is expected to be patterned by chemical etching because the volatile etch product can be produced [8,9].

Even though there are some reports on the basic characteristics of Ru etching using various plasma

sources such as electron cyclotron resonance plasma, helicon plasma [10], and inductively coupled plasma [11], there are rare report on the study of Ru etching using reactive ion etcher (RIE).

In this study, we report the etching characteristics of Ru using O<sub>2</sub>/Cl<sub>2</sub> plasmas in dual frequency RIE tool. We investigate the Ru etch rate and the Ru to SiO<sub>2</sub> mask etch selectivity with varied process conditions including pressure, RF power, total gas flow rate. We also evaluate the effect of substrate temperature on the Ru etch rate and etching profile by varying the chiller temperature.

## 2. Experiments

The sample structure was Si substrate/TiN 600 Å/Ru 4000 Å/SiO<sub>2</sub> mask. SiO<sub>2</sub> mask, instead of photoresist (PR) mask, was used for patterning

\*Corresponding author. Tel.: +82-32-860-7544; fax: +82-32-862-5546.

E-mail address: [hwkim@inha.ac.kr](mailto:hwkim@inha.ac.kr) (H.W. Kim).

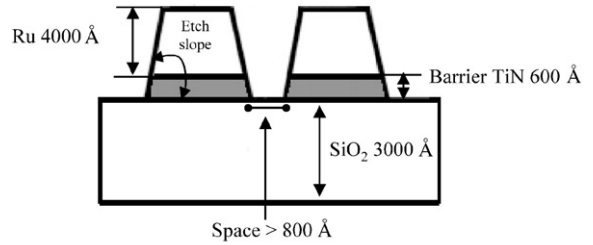
Ru, because oxygen gas was the main etchant in our experiments. The SiO<sub>2</sub> mask was patterned by CF<sub>4</sub>/N<sub>2</sub>/Ar gas. After patterning SiO<sub>2</sub>, the PR mask was removed. A storage node pattern was used in our experiments. Top view of the storage node pattern indicates that the storage node is an oval type.

Schematic of a reactive ion etcher (RIE) for Ru etching is shown in our previous report [12]. A dual frequency Tegal 6540 RIE tool commercially available from Tegal, Inc. has been used. The combination of high RF (HRF) power (13.56 MHz) and low RF (LRF) power (450 kHz) results in high-energy ion bombardment. The wafer substrate temperature during etching was controlled by chiller and the chiller temperature was varied from 25°C to 220°C. The Ru etch process consists of a main etch step stopped at end point detection (EPD) and an over etch step to remove the Ru residues. Then the barrier TiN layer was removed by etching with Ar and Cl<sub>2</sub> gases.

After removing TiN barrier layer, the bottom space between two adjacent nodes should be wider than 80 nm, because the following steps of the BST deposition (estimated to be ≥300 Å in thickness per side) and the top electrode Ru deposition need to be accomplished in order to fabricate the Ru/BST/Ru capacitor. At the same time, the top width of the storage node should be maintained without reduction by erosion, to ensure a sufficient capacitance area and thus satisfy a required storage capacity per cell. For example, the required Ru etch slope at the critical dimension (CD) of 0.15 μm is calculated to be 86° (Fig. 1).

As Ru cannot be etched by halogen gases due to high boiling point of their etch products, we used O<sub>2</sub> gas as a main etchant, expecting that the volatile RuO<sub>4</sub> is produced [9,10]. The Cl<sub>2</sub> gas was added to enhance the etch rate. The additive gases including Cl<sub>2</sub> gas is known to increase the etch rate of RuO<sub>2</sub> by increasing the concentration of oxygen radicals [13] and it is surmised that the etchant radicals react with RuO<sub>2</sub>, forming the volatile RuO<sub>4</sub> [14].

A scanning electron microscope (SEM) was used to measure the Ru etching slope and the etch rates of Ru and SiO<sub>2</sub>. As shown in Fig. 2, the Ru



CD (μm)	0.29	0.20	0.17	0.15
Required Etch slope	> 77°	> 83°	> 85°	> 86°

Fig. 1. The required Ru etching slope for the fabrication of Ru/BST/Ru capacitor.

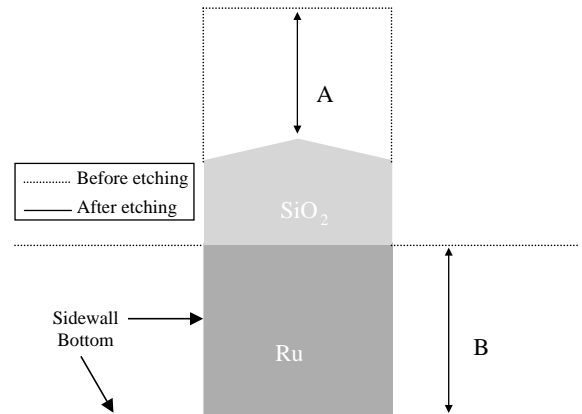


Fig. 2. The calculation of Ru to SiO<sub>2</sub> etches selectivity (B/A).

to SiO<sub>2</sub> etch selectivity is calculated to be B/A in this work. In order to prepare a sample for SEM observation, a wafer was cut along the short axis of storage node patterns.

### 3. Results and discussions

We applied a Ru etching technique to stacked storage node pattern with a CD of 0.17 μm, with an expectation to apply the technique into future devices. Fig. 3 shows the change of Ru etch rate, SiO<sub>2</sub> etch rate, and the Ru to SiO<sub>2</sub> etch selectivity by varying the pressure and the total gas flow rate. The HRF power, LRF power, and the

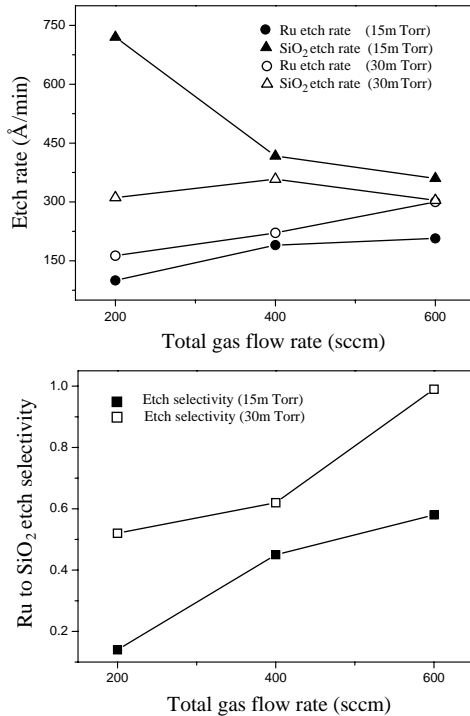


Fig. 3. Change of Ru etch rate, SiO<sub>2</sub> etch rate, and the Ru to SiO<sub>2</sub> etch selectivity by varying the pressure and the total gas flow rate.

Cl<sub>2</sub>/(O<sub>2</sub> + Cl<sub>2</sub>) gas flow rate were set to 700 W, 0 W, and 0.2, respectively. In case of 15 mTorr (2 Pa), when the total gas flow rates are 200, 400, and 600 sccm, respectively, the Ru etch rates are 100, 190, and 207 Å/min and the SiO<sub>2</sub> etch rates are 720, 417, and 360 Å/min. In case of 30 mTorr (4 Pa), when the total gas flow rates are 200, 400, and 600 sccm, respectively, the Ru etch rates are 163, 221, and 300 Å/min and the SiO<sub>2</sub> etch rates are 311, 358, and 304 Å/min. We reveal that the Ru etch rate and thus the Ru to SiO<sub>2</sub> etch selectivity increase by increasing the total gas flow rate regardless of pressure. We also reveal that the Ru etch rate and thus the Ru to SiO<sub>2</sub> etch selectivity increase by increasing the pressure regardless of the total gas flow rate. Since the Ru etching reaction is favored at higher pressure and higher total gas flow rate, we surmise that chemical reaction plays a role in the Ru etching and it agrees with the previous report [10,14].

In order to evaluate the effect of HRF power and LRF power, we have changed the HRF power from 700 to 500 W and the LRF power from 100 to 0 W. Fig. 4 shows the change of Ru etch rate, SiO<sub>2</sub> etch rate, and the Ru to SiO<sub>2</sub> etch selectivity by varying the HRF power and the LRF power. The pressure, the O<sub>2</sub> flow rate, and Cl<sub>2</sub> flow rates, respectively, are set to 30 mTorr, 480, and 120 sccm. When the HRF power decreases from 700 to 500 W, the Ru etch rate increases from 120 to 170 Å/min. When the LRF power decreases from 100 to 0 W, the Ru etch rate increases from 120 to 300 Å/min. However, the SiO<sub>2</sub> etch rate does not change by varying the HRF power and the LRF power. When the HRF power decreases from 700 to 500 W, the Ru to SiO<sub>2</sub> etch selectivity increases from 0.33 to 0.57. When the LRF power decreases from 100 to 0 W, the Ru to SiO<sub>2</sub> etch selectivity increases from 0.33 to 0.99. It is noteworthy that Ru etch rate decreases by increasing the RF powers. We surmise that the

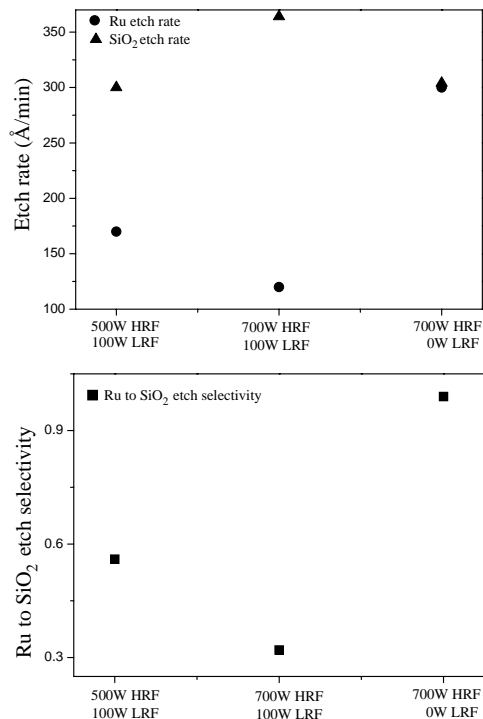


Fig. 4. Change of Ru etch rate, SiO<sub>2</sub> etch rate, and the Ru to SiO<sub>2</sub> etch selectivity by varying the HRF power and the LRF power.

chemical reactions thus the radical plays a crucial role in the Ru etching using  $O_2/Cl_2$  plasma and the relative amount of radical decreases and that of ions increases by increasing the RF power. In case of small-CD pattern, some sputtered Ru atoms cannot escape from the valley and are reattached onto the Ru sidewall. Furthermore, the accelerated ions sputters Ru atoms in the sidewall into the bottom surface of Ru film. Further studies are necessary to reveal the detailed mechanism.

In order to evaluate the effect of temperature, we have changed the chiller temperature from  $80^\circ C$  to  $220^\circ C$ . The HRF power, LRF power, pressure,  $O_2$  flow rate, and  $Cl_2$  flow rate were set to 600, 100 W, 30 mTorr, 80, and 20 sccm. Fig. 5 shows the change of Ru etch rate,  $SiO_2$  etch rate, and the Ru to  $SiO_2$  etch selectivity by varying the chiller temperature. When the chiller temperature increases from  $80^\circ C$  to  $220^\circ C$ , the Ru etch rate increases from 50 to  $185 \text{ \AA}/\text{min}$  thus the Ru to  $SiO_2$  etch selectivity increases from 0.28 to 1.01.

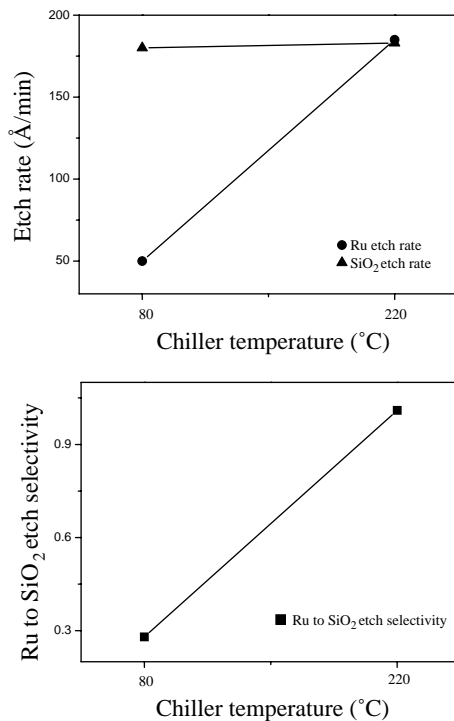


Fig. 5. Change of Ru etch rate,  $SiO_2$  etch rate, and the Ru to  $SiO_2$  etch selectivity by varying the chiller temperature.

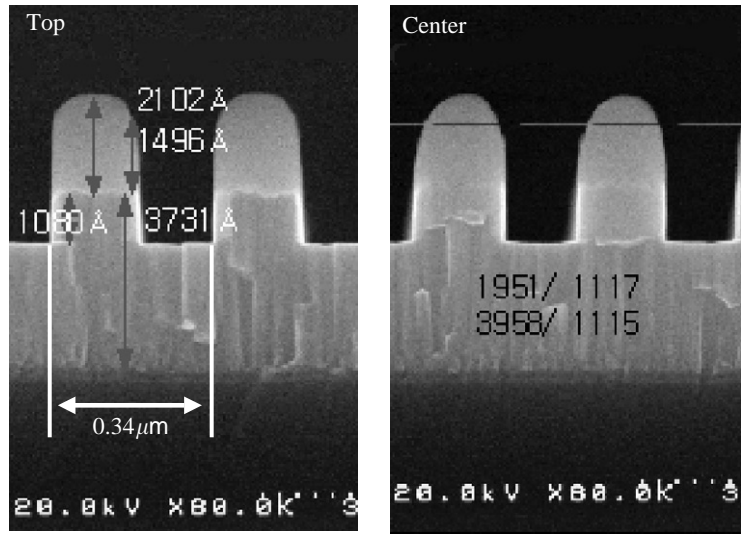
While the  $SiO_2$  etch rate does not depend on the chiller temperature, the Ru etch rate increases by increasing substrate temperature. We surmise that elevating the substrate temperature helps to proceed the chemical etching and it agrees with the previous result indicating that the  $RuO_4$  is a main etching product and the generation of  $RuO_4$  is favorable at higher temperature [14].

We have revealed that the Ru etch rate and thus the Ru to  $SiO_2$  etch selectivity increase by increasing pressure, total gas flow rate, temperature and decreasing HRF power and LRF power. We have applied the standard condition in which the pressure, HRF power, LRF power, total gas flow rate, and the chiller temperature were set to 30 mTorr, 500, 100 W, 600 sccm, and  $220^\circ C$ , respectively. The Ru etch rate and the  $SiO_2$  etch rate are 220 and  $160 \text{ \AA}/\text{min}$ , respectively. Fig. 6 shows the vertical cross section of the storage node bottom electrode, along the short-axis. Fig. 6b reveals that the Ru etching profile has a slope of  $90^\circ C$  after etching with a 30%-overetch. The vertical profile does not result from the overetching, because the partial etching also shows the vertical profile during etching (Fig. 6a). Fig. 6a indicates that the etch uniformity is less than 5%, which is acceptable to sub-micron technologies.

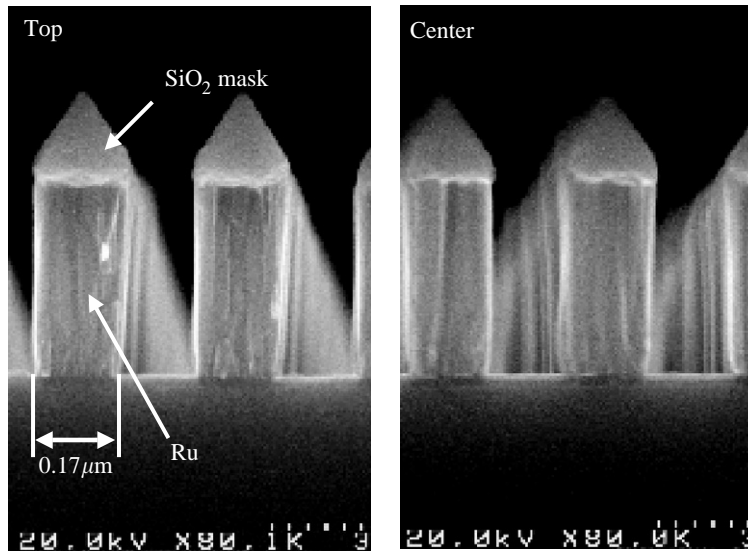
In his work, we have succeeded in obtaining the completely vertical Ru etching profile by employing the reactive ion etching method. However, the Ru etch rate is lower than using ICP reactor being reported in our previous experiments [11]. The detailed mechanism of Ru etching should be revealed to seek a possibility of obtaining the high etch rate and the vertical profile simultaneously.

#### 4. Conclusions

We investigate the characteristics of Ru electrode etching using  $O_2/Cl_2$ -based plasma in reactive ion etcher. We have revealed that the Ru etch rate and thus the Ru to  $SiO_2$  etch selectivity increase by increasing pressure, total gas flow rate, temperature. The RF powers need to be optimized to prevent excessive ion bombardment. For the



(a)



(b)

Fig. 6. SEM micrographs of Ru etching profile using the standard condition, revealing that the vertical profile is attained: (a) Before end point detection (about 30% of EPD duration) (b) 30%-overetched after EPD. The left-hand side and the right-hand side of figures represent the etching profile of the top and the center part of the wafer, respectively.

first time we have reported the Ru etching profile with an etching slope of  $90^\circ$  at a CD of  $0.17\ \mu\text{m}$ . Since obtaining the vertical profile is possible, the Ru etching technique will be applicable to the very small CD-pattern below  $0.15\ \mu\text{m}$ .

### Acknowledgements

This work was supported by Inha University Research Grant through the Special Research Program in 2002 (INHA-22524).

**References**

- [1] Yamamichi S, Lesaicherre PY, Yamaguchi H, Takemura K, Sone S, Yabuta H, Sato K, Tamura T, Nakajima K, Ohnishi S, Tokashiki K, Hayashi Y, Kato Y, Miyasaka Y, Yoshida M, Ono H. *IEDM Tech Dig* 1995;119.
- [2] Yuuki A, Yamamuka M, Makita T, Horikawa T, Shibano T, Hirano N, Maeda H, Mikami N, Ono K, Ogata H, Abe H. *IEDM Tech Dig* 1995;115.
- [3] Lee BT, Lee KH, Hwang CS, Kim WD, Horii H, Kim HW, Cho HJ, Kang CS, Chung JH, Lee SI, Lee MY. *IEDM Tech Dig* 1995;249.
- [4] Aoyama T, Yamazaki S, Imai K. *J Electrochem Soc* 1998;145:2961.
- [5] Yoo WJ, Hahm JH, Kim HW, Jung CO, Koh YB, Lee MY. *Jpn J Appl Phys* 1996;35:2501–4.
- [6] Nishikama K, Kusumi Y, Oomori T, Hanazaki M, Namba K. *Jpn J Appl Phys* 1993;32:6102.
- [7] Yokoyama S, Ito Y, Ishihara K, Hamada K, Ohnishi S, Kudo J, Sakiyama K. *Jpn J Appl Phys* 1995;34:767.
- [8] Saito S, Kuramasu K. *Jpn J Appl Phys* 1992;31:135.
- [9] Pan W, Desu SB. *J Vac Sci Technol B* 1994;12:3208.
- [10] Kim HW, Han JH, Ju BS, Kang CJ, Moon JT. *Mater Sci Eng B* 2002;95:249–53.
- [11] Kim HW, Ju BS, Kang CJ. *Microelectron Eng* 2003;6J:319.
- [12] Kim HW, Ju BS, Nam BY, Yoo WJ, Kang CJ, Ahn TH, Moon JT, Lee MY. *J Vac Sci Technol A* 1999; 17:2151–5.
- [13] Lee EJ, Kim JW, Lee WJ. *Jpn J Appl Phys* 1998;37:2634.
- [14] Tokashiki K. *Proceedings of SEMI Technology Symposium*, 1996. p. 5–46.